State selection in a cesium beam by laser-diode optical pumping

G. Avila,* V. Giordano, V. Candelier,† E. de Clercq,‡ G. Theobald, and P. Cerez§
Laboratoire de l'Horloge Atomique, Bâtiment 221, Université Paris-Sud, 91405 Orsay, France
(Received 9 February 1987)

In this paper the optical pumping of a cesium beam is investigated. The rate equation model is used to calculate the population difference created by laser diode(s) illuminating the beam. The finite laser and atomic linewidths are taken into account in order to analyze leakage effects on neighboring transitions. One-laser and two-laser pumping is considered and the best-suited two-laser configurations for preparing the cesium atoms in a single $m_F=0$ sublevel are specified. Experimental results on both the leakage effect and the population difference achieved agree with theoretical predictions.

I. INTRODUCTION

The use of laser optical pumping to prepare alkali-metal-atom beams in well-defined quantum states is of current interest. Such polarized atomic beams are useful in different areas of nuclear and atomic physics: production of polarized ion sources,[1] investigation of atomic scattering processes,[2] spectroscopy,[3] production of Rydberg states in alkali-metal atoms,[4] laser cooling of neutral atoms,[5–8] and measurement of atomic parity violation.[9] The D_2-line optical pumping of cesium atoms can be performed efficiently with tunable laser diodes at the appropriate wavelength around 852 nm.[10] The process results in the transfer of atoms out of one of the two ground-state hyperfine levels. In the field of atomic frequency standards, this technique was proposed for replacing the magnetic state selection method in which an inhomogeneous magnetic field is used to deflect cesium atoms in a beam.[11,12] In that case, a population difference between the $F=3$, $m_F=0$, and $F=4, m_F=0$ levels of the ground state must be created. A qualitative explanation of the optical pumping process involved is the following. Due to the arrangement of the cesium hyperfine levels, shown in Fig. 1(a), an incident linearly polarized laser light is absorbed by the atoms causing $F'-F=0,\pm1$ transitions with $\Delta m_F=0$ or ±1 depending on whether the laser light is π or σ polarized. Thus the light brings atoms from one of the two F ground-state hyperfine levels to an F' excited one. Once atoms are in the excited level, they decay by spontaneous emission to one of the two ground-state levels. After many cycles of absorption followed by spontaneous emission, atoms are transferred from one ground-state level to another one and a population difference between the $m_F=0$ ground-state sublevels is achieved. However, in the case of a single laser pumping, only a fraction of the atoms is available for the microwave $\Delta F=1, m_F=0$ transition. The creation of a larger population difference requires absorption from both ground-state hyperfine levels, using two lasers for instance.[13] It is even possible to accumulate all atoms of the beam in a single $m_F=0$ sublevel.[14]

Although the validity of this optical pumping scheme was experimentally verified, fundamental questions arise and several experimental constraints have to be taken into account for an accurate determination of the optical pumping efficiency.

(i) Effective optical pumping requires that the product of light intensity times the light-atom interaction time is sufficiently large so that many cycles of absorption–spontaneous emission occur. Consequently it is important to know if the available laser intensity is sufficient to ensure complete optical pumping and if not, to determine what transitions are the more quickly pumped.

(ii) There are two optical transitions, the $F=3\rightarrow F'=2$ and the $F=4\rightarrow F'=5$ ones, which cannot give rise to hyperfine optical pumping because each realizes a two-level quantum system. It follows that atoms cannot be transferred from one ground-state hyperfine level to another one. These transitions, called "cycling" or "closed" transitions, are of limited interest for pumping purpose. However, we shall show that Zeeman pumping[11] creates a weak population difference. Fur-

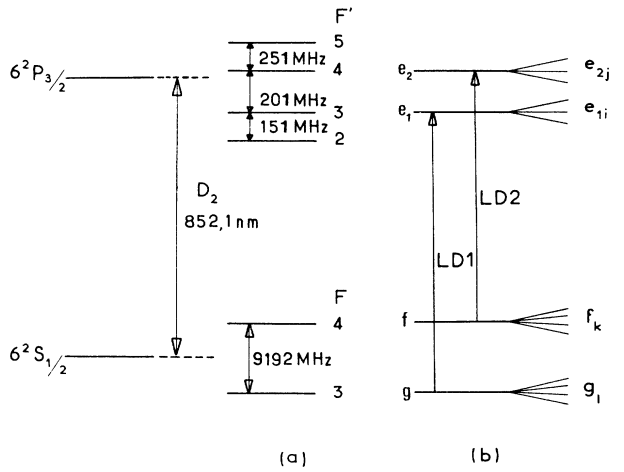

FIG. 1. Energy-level diagram corresponding to the D_2 line of cesium atom. (a) Fine and hyperfine structure. (b) Laser excitation considered. The energy gaps are not to scale.

thermore, their high level of fluorescence brings valuable improvement of the optical detection process.[13]

(iii) No matter which particular transitions are involved, two-laser pumping is more efficient than one-laser pumping to create a population difference between the $m_F=0$ sublevels in the ground state. Nevertheless, several conditions must be fulfilled in order to obtain the best pumping efficiency: they are related to the laser intensity, the interaction time, and the appropriate choice of the involved optical transitions.

(iv) When the laser is tuned to a given optical transition, leakages occur because neighboring transitions, located 151, 201, or 251 MHz away from the main line, can be simultaneously excited. This effect is made possible because the laser-diode spectrum has a Lorentzian line shape with a finite width, usually of the order of 25 MHz, and the laser spectrum wing overlaps neighboring lines with a small but non-negligible amplitude. Since atoms are lost during the pumping cycle, the pumping efficiency could be appreciably affected.

The subject of the present paper is to study both theoretically and experimentally the efficiency of optical pumping applied to the preparation of cesium atoms in a single $m_F=0$ sublevel. In order to discuss the optical pumping in a cesium atomic beam we first present the theoretical model used to predict the evolution of the populations. Then, in Sec. II, we give the expected performances in the one-laser and the two-laser pumping schemes. We study the leakage mechanism and its influence on the optical pumping efficiency in Sec. III. The experimental setup is briefly described in Sec. IV. It gives the variation of the fluorescence signal recorded when state selected atoms undergo the microwave $\Delta F=1, \Delta m_F=0$ transition.[15] This technique allows for a sensitive control of the preparation of the cesium atomic beam. In Sec. V a comparison between the theoretical predictions and the experimental results is made with two basic aims: firstly to make clear the influence of population leakages and secondly to identify the best-suited transitions for atomic cesium beam preparation.

II. THEORETICAL MODEL

Our concern is to follow the time evolution of the atomic populations in the ground state. Since we consider large linewidth lasers and weak laser intensities, the rate equation approach can be used to solve the present problem.[16]

The energy levels of the $6\,^2S_{1/2}$ ground state and of the $6\,^2P_{3/2}$ excited state of the cesium atom are shown in Fig. 1. Optical pumping is carried out by one- or two-laser diodes LD1 and LD2. The laser light source LD1 is tuned to produce an optical transition from the $F=3$ hyperfine multiplet to the $F'=e_1$ excited one. Similarly, LD2 excites the transition between the $F=4$ and $F'=e_2$ multiplets [see Fig. 1(b)]. According to the selection rules, the quantum number F' of the excited states is such that we have $F'-F=0$ or ± 1. Since the spectral laser linewidth, which is of the order of 25 MHz, is larger than the natural width of the D_2 lines, equal to 5 MHz, the model assumes that within a hyperfine manifold all Zeeman sublevels interact with optical pumping light equally. Furthermore it is assumed, for simplicity, that the cesium beam is monokinetic.

The following general relationships hold for the populations $n_{e_{1i}}, n_{e_{2j}}$ and n_{f_κ}, n_{g_l} of the excited- and ground-state sublevels, respectively:

$$
\begin{aligned}
\frac{dn_{e_{1i}}}{dt} &= \sum_l W_{g_l\to e_{1i}} n_{g_l} - \sum_l W_{e_{1i}\to g_l} n_{e_{1i}} - \Gamma n_{e_{1i}} , \\
\frac{dn_{e_{2j}}}{dt} &= \sum_k W_{f_k\to e_{2j}} n_{f_k} - \sum_k W_{e_{2j}\to f_k} n_{e_{2j}} - \Gamma n_{e_{2j}} , \\
\frac{dn_{f_k}}{dt} &= -\sum_j W_{f_k\to e_{2j}} n_{f_k} + \sum_j W_{e_{2j}\to f_k} n_{e_{2j}} \\
&\quad + \sum_j A_{e_{2j}\to f_k} n_{e_{2j}} + \sum_i A_{e_{1i}\to f_k} n_{e_{1i}} , \\
\frac{dn_{g_l}}{dt} &= -\sum_i W_{g_l\to e_{1i}} n_{g_l} + \sum_i W_{e_{1i}\to g_l} n_{e_{1i}} \\
&\quad + \sum_i A_{e_{1i}\to g_l} n_{e_{1i}} + \sum_j A_{e_{2j}\to g_l} n_{e_{2j}} ,
\end{aligned}
\tag{1}
$$

where the subscripts i and j take $2F'+1$ values associated with the quantum number F' of the excited state considered. The same rule applies to k and l. The W coefficients are stimulated emission or absorption rates. They are related to the spontaneous emission rates A by

$$
W_{e_{1i}\to f_k} = W_{f_k\to e_{1i}} = \frac{3}{4}\frac{\lambda^3}{\pi^2 hc}\frac{I}{\Delta\nu_L} A_{e_{1i}\to f_k} \epsilon_q^2 , \tag{2}
$$

where $q=i-k$ takes the values $+1$, -1, and 0. ϵ_q is the component of the polarization vector along the σ^+, σ^-, and π vectors. h is Planck's constant, c the speed of light in vacuum, and I the laser intensity expressed in $\mathrm{W\,m^{-2}}$. The laser wavelength λ is equal to 852 nm and the laser linewidth $\Delta\nu_L$ to 25 MHz. The spontaneous emission rates A are proportional to the spontaneous emission decay rate Γ.[17] They are given in Appendix A.

In the case of two-laser pumping, the set of equations (1) represents $(2e_2+1)+(2e_1+1)+16$ simultaneous equations. In the particular case where the excited levels of the two-laser scheme are the same, we have $e_1=e_2$. Equations (1) must be modified as indicated in Appendix B and the number of equations becomes $(2e_1+1)+16$. When only one laser is used for the pumping, the number of equations is equal to $(2e_1+1)+16$ or $(2e_2+1)+16$ depending on whether LD1 or LD2 illuminates the beam.

The coupled rate equations (1) have been solved numerically with the initial condition that all ground-state sublevels are equally populated and that all the excited levels are depleted.

A. Case of one-laser pumping

The time-dependent results are shown in Fig. 2 for $I=10$ mW cm^{-2} and for several laser tunings and polarizations.[18] The fractional population difference Δn of the $m_F=0$ ground-state hyperfine sublevels is defined as

$$\Delta n=\frac{n(F=4,m_F=0)-n(F=3,m_F=0)}{n}, \quad (3)$$

where n is the total population of the cesium ground- and excited-state levels. Δn reaches quickly a steady-state value and an almost complete depopulation of one of the two $m_F=0$ sublevels is achieved after a light-atom interaction time of about 3 μs, except for the $(4\rightarrow 4,\pi)$ and the $(3\rightarrow 3,\pi)$ schemes. In these two cases $F'-F=0$ transitions occur and, whatever the laser intensity may be, none of the $m_F=0$ sublevels can be depopulated because the transition probability is zero for $F'-F=0$, $m_F=0$ transitions. The conclusions concerning the best pumping efficiency are the same as mentioned in Ref. 19: with a σ-polarized light, Δn reaches -15.5% and -15.4% for the $F=4\rightarrow F'=4$ and $F=4\rightarrow F'=3$ transitions, respectively; with a π-polarized light, the highest value of Δn is obtained for the $F=3\rightarrow F'=4$ transition.

The particular behavior of the cycling transitions for which Zeeman pumping[11] occurs should be noted. The total population of the starting ground-state level does not vary. Nevertheless, the final distribution of the atoms among the Zeeman sublevels of this ground state is modified and the fractional population difference Δn between the $m_F=0$ sublevels, although weak, is not negligible. This is especially true for the $F=4\rightarrow F'=5$ transition.

B. Case of two-laser pumping

Several two-laser schemes can be used in order to increase very significantly the 0-0 population difference.[14] They are listed in Fig. 3. These schemes are chosen in the following way. A first laser populates one of the F ground-state levels. A second laser, π polarized, tuned to the $F'-F=0$ transition, depletes all the ground-state sublevels except the $F,m_F=0$ one, according to the transition probabilities.[19] It is worth noting that one of the lasers must be tuned to an optical $\Delta F=0$ transition and π polarized in order to achieve an efficient population transfer to a $m_F=0$ ground-state sublevel.

Figure 3 shows for all the possible schemes the evolution of the absolute value of Δn as a function of time when the laser intensity is equal to 3 mW cm^{-2}. Several important features of the two-laser pumping are clearly illustrated.

(i) The population difference Δn becomes important when the interaction time is sufficiently large; in this respect, the most efficient pumpings make use of the $(3\rightarrow 3,\pi;4\rightarrow 4,\sigma)$ and of the $(3\rightarrow 3,\pi;4\rightarrow 3,\sigma)$ schemes for which Δn reaches -89.1% and -84.2%, respectively, when the interaction time is equal to 20 μs.

(ii) It is to be noted that the $(3\rightarrow 3,\pi;4\rightarrow 3,\pi)$ and the $(3\rightarrow 3,\pi;4\rightarrow 4,\pi)$ configurations cannot reach a 50% fractional population difference. The first one piles up a part of the atoms into the $F=4,m_F=\pm 4$ sublevels because the $F=4,m_F=\pm 4\rightarrow F'=3,m_F=\pm 3$ transitions are forbidden; the second configuration fills up simultaneously the $F=4,m_F=0$ and $F=3,m_F=0$ sublevels. However, the final population difference Δn is still significant, being equal to -46% and -33%, respectively.

(iii) Lastly, comparison with Fig. 2 shows that a longer interaction time is needed to approach closely the steady state. Most of the two-laser schemes have not yet achieved a complete pumping when the interaction time is 20 μs. In order to estimate the time required to achieve an almost complete optical pumping, let us define a pumping time T_p as the time interval necessary to obtain a value of $|\Delta n|$ equal to 90%. Figure 4

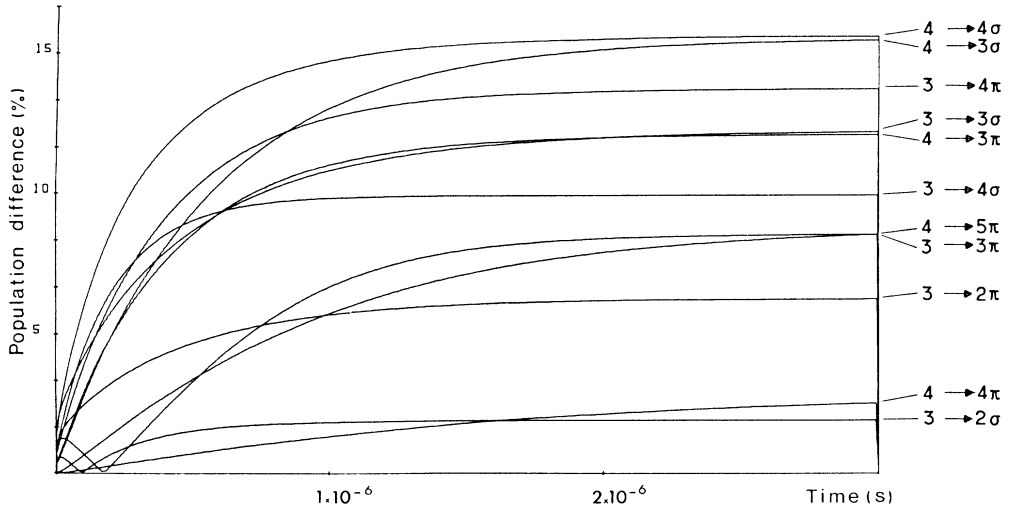

FIG. 2. Time evolution of the absolute value of the fractional population difference Δn between the $m_F=0$ ground-state sublevels. Optical pumping is performed with one laser. $I=10$ mW cm^{-2}.

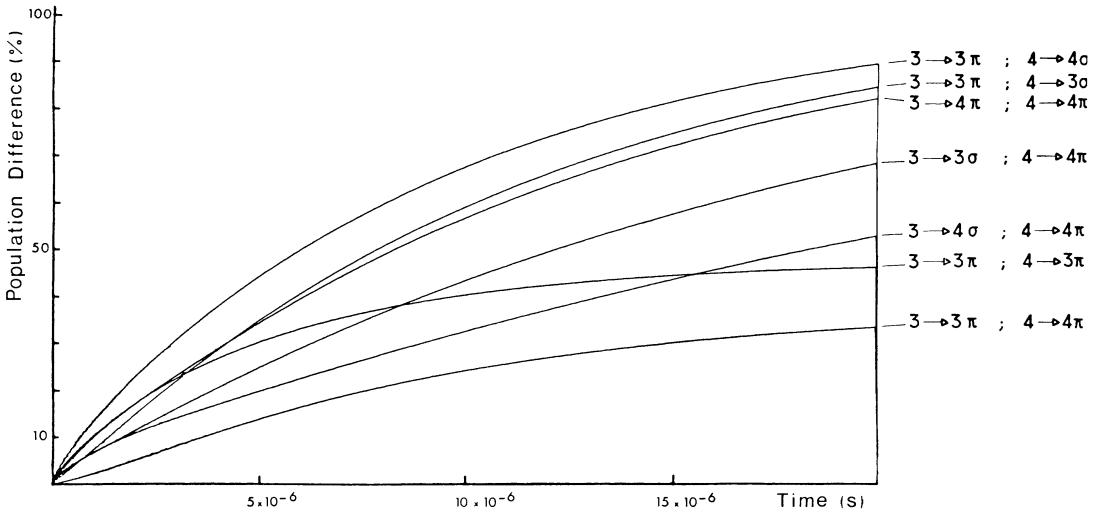

FIG. 3. Time evolution of the absolute value of Δn in the case of two-laser optical pumping. $I=3$ mW cm^{-2} for each laser.

shows the variation of T_p in the $(3\rightarrow 3,\pi;4\rightarrow 4,\sigma)$ scheme, for instance, as a function of the laser intensity I delivered by each laser. T_p shows a rapid decrease followed by a slow variation as I increases. If the time spent by the atoms in the laser light is 20 μs, a laser intensity of 3 mW cm^{-2} is already sufficient to perform an efficient pumping. However, in most of the other two-laser schemes, namely, the $(3\rightarrow 4,\pi;4\rightarrow 4,\pi)$, $(3\rightarrow 3,\sigma;4\rightarrow 4,\pi)$ and $(3\rightarrow 4,\sigma;4\rightarrow 4,\pi)$ ones, the pumping time T_p is notably increased. We conclude that the two best pumping schemes are those mentioned in (i) above, i.e., the $(3\rightarrow 3,\pi;4\rightarrow 4,\sigma)$ and the $(3\rightarrow 3,\pi;4\rightarrow 3,\sigma)$ configurations.

III. POPULATION LEAKAGES

So far we have ignored the possibility of exciting neighboring transitions when the laser is tuned to a given atomic transition.[20] As the laser power spectrum is Lorentzian with a linewidth of about 25 MHz, optical excitation is expected even far from the laser line center and a leakage of atoms on excited levels 151, 201, or 251 MHz away becomes possible. In order to analyze the effect of these leakages on the pumping efficiency, the rate equation model can be modified to include the case when two transitions share in common the same ground-state level, the level $F=3$ in the example shown in Fig. 5. The basis for further calculations now lies in the determination of the relative absorption and stimulated emission rates W_f when the atomic line is far from the center line.[21] If $g_A(\nu-\nu_A)$ and $g_L(\nu-\nu_L)$ are, respectively, the Lorentzian atomic and laser line shapes centered at frequencies ν_A and ν_L, then, the rates W_f are related to the spontaneous emission rates A by

$$W_f=\tfrac{3}{8}\frac{\lambda^3}{\pi hc}IA\int_{-\infty}^{+\infty} g_A(\nu-\nu_A)g_L(\nu-\nu_L)d\nu \ . \quad (4)$$

Consequently, they are related to the absorption rates W defined in Sec. II in the case of a very small atomic linewidth by the relation

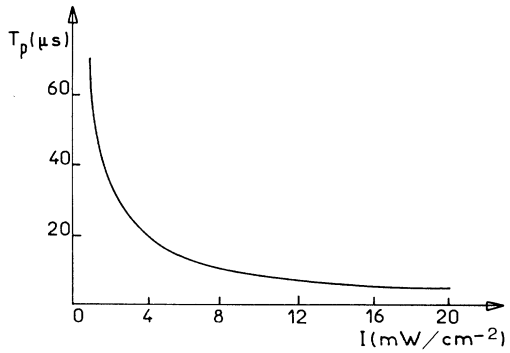

FIG. 4. Pumping time as a function of the intensity of the two pumping lasers in the $(3\rightarrow 3,\pi;4\rightarrow 4,\sigma)$ scheme.

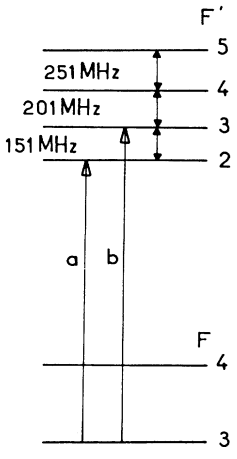

FIG. 5. A leakage on the (b) transition can occur when the laser is tuned to the (a) transition.

TABLE I. Absorption rates W_f of atomic transitions in the case of finite atomic and laser linewidths. $\nu_A-\nu_L$ is the position of the transition measured from the center laser line (in MHz). The W rates are defined in Sec. II assuming that the atomic linewidth is very small.

$\nu_A-\nu_L$	0	150	200	250
W_f/W	0.85	1.16×10^{-2}	6.5×10^{-3}	4.1×10^{-3}

$$W_f = Wm(m+1)\frac{t_0^2+(m-1)^2}{(t_0^2+m^2-1)^2+4t_0^2}\ , \tag{5}$$

where $m=2\pi\Delta\nu_L/\Gamma$ denotes the ratio of the laser and atomic linewidths and $t_0=4\pi(\nu_A-\nu_L)/\Gamma$ represents the position of the atomic linewidth measured from the center of the laser line. The values of W_f/W are given in Table I for each relevant detuning and it is evident that simultaneous excitation of the $F=3\rightarrow F'=3$ and of the $F=3\rightarrow F'=2$ transitions may be effective.

IV. EXPERIMENTAL RESULTS

The population difference of the two $m_F=0$ ground-state sublevels is observed by means of the fluorescence light variation when atoms undergo the microwave transition at 9192 MHz. A schematic of the experimental setup is shown in Fig. 6. The cesium beam is optically pumped in the first region and the fluorescence induced by the linearly polarized laser beam is used for laser frequency locking purposes. The microwave transition $\Delta F=1, \Delta m_F=0$ is induced in a two-arms Ramsey cavity and is detected in the third region through atomic beam fluorescence variations. Pumping may be. performed with one or two lasers whereas detection is accomplished with one laser.

The separation between the oven and the detection region is 53 cm. The oven's collimator consists of a stack of crinkled foils. Its cross section is 4×2 mm^2. The beam cross section in the detection region is 11×4 mm^2 in order to ensure a large signal. A single cylindrical magnetic shield made of μ-metal surrounds the Ramsey cavity and the two light-beam interaction regions. Four current-carrying rods produce a vertical static field usually called the C field.

The distance between the two arms of the U-shaped waveguide cavity is 21.5 cm, thus giving a Ramsey pattern microwave resonance width of about 500 Hz.

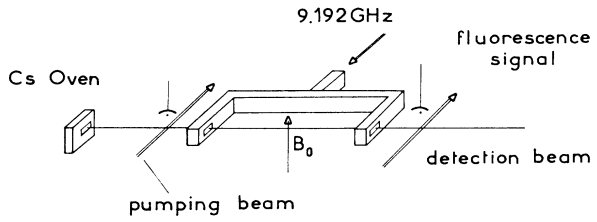

FIG. 6. Schematic representation of our optically pumped cesium beam machine.

Light-atom interaction zones are identical and designed in order to minimize the scattered laser light. Microwave transitions are detected in the second light-beam interaction region by means of a large area (1 cm^2) and low-noise silicon photodiode.

The light sources are single-frequency Ga-Al-As Hitachi HLP 1400 laser diodes operating around 852 nm with an optical power of a few milliwatts. The rough adjustment of the wavelength is achieved through the temperature which is controlled to a few mK using a thermoelectric cooler.

We have shown in Sec. II that in a two-laser pumping scheme the π polarization of the laser tuned to a $F'-F=0$ transition is a necessary condition for accumulating atoms in a single $m_F=0$ ground-state sublevel. Consequently, improper polarization may reduce drastically the population difference of interest. This effect was measured as a function of the laser polarization θ and it is reported in Fig. 7. The behavior of the experimental curve is essentially as expected from calculations made with the rate equation model. When θ is equal to 5°, Δn decreases from 1 to 0.8. Therefore a slight misalignment of the laser polarization can significantly reduce the signal.

In a two-laser experiment, the available intensity of each laser was 3 mW cm^{-2}. According to the theoretical results of Fig. 4, this intensity is almost sufficient to achieve complete pumping. This fact is supported by the record of the microwave resonance signals shown in Figs. 8(a) and 8(b). Figure 8(a) has been obtained by using a single laser, tuned to the $F=4\rightarrow F'=3$ transition and σ polarized, for optical pumping and for optical detection. The seven $\Delta F=1$, $\Delta m_F=0$ transitions are clearly visible. In Fig. 8(b) the optical pumping and the optical detection have been performed using the $(3\rightarrow3,\pi;4\rightarrow3,\sigma)$ and the $(4\rightarrow3,\sigma)$ configurations, respectively. In that case the central ($m_F=0$) line is greatly enhanced, whereas only the two nearest field-

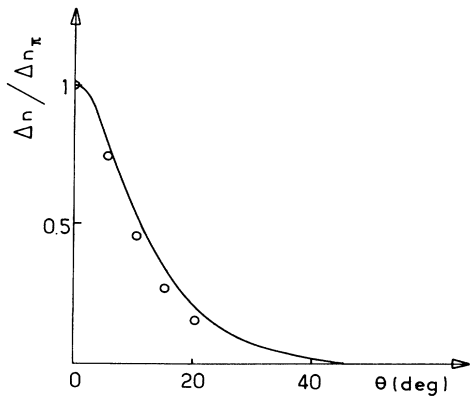

FIG. 7. Relative decrease of the population difference as a function of the polarization θ of one laser. The two-laser pumping uses the $(3\rightarrow4,\pi;4\rightarrow4,\pi+\theta)$ scheme. Δn_π is the population difference at $\theta=0°$. The solid curve refers to the results of the rate equation model and circles to the experimental values.

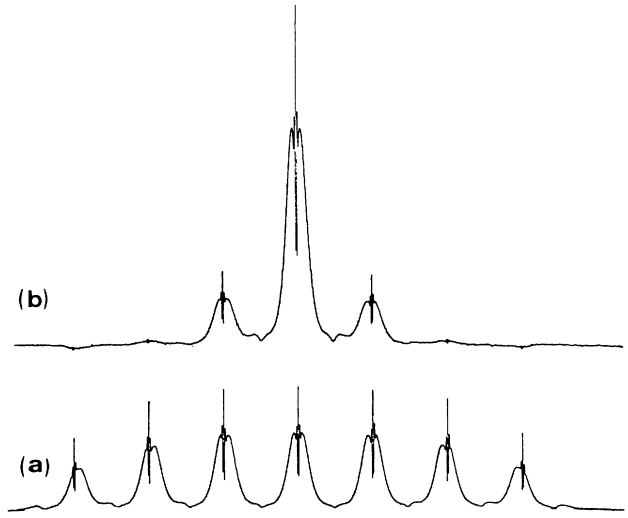

FIG. 8. Experimental recorded microwave spectrum. (a) A single laser tuned to the $F=4\rightarrow F'=3$ transition and σ polarized is used for the optical pumping and the optical detection. (b) The optical pumping and the optical detection are performed using the $(3\rightarrow 3,\pi;4\rightarrow 3,\sigma)$ and the $(4\rightarrow 3,\sigma)$ configurations, respectively.

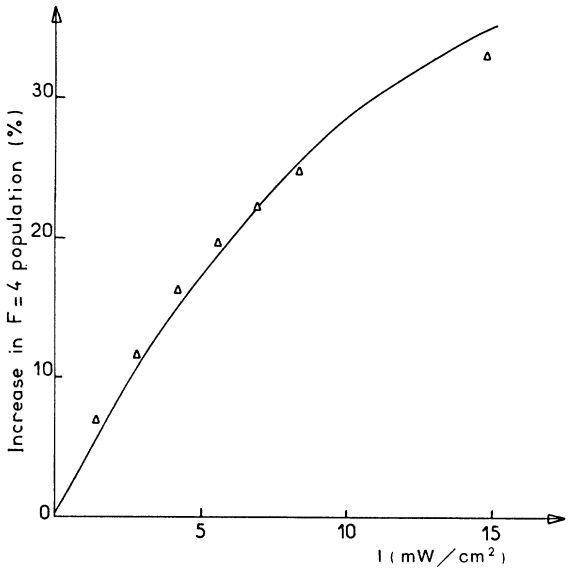

FIG. 9. Relative increase of the $F=4$ population vs the laser intensity. The laser is tuned to the $F=3\rightarrow F'=2$ transition. Solid curve: calculation with the rate equation model. Triangles: experimental points.

dependent lines are still present, but with a weak amplitude.

V. COMPARISON OF THEORETICAL AND EXPERIMENTAL RESULTS

Firstly we shall analyze the leakage effect and secondly the pumping efficiency.

A. Leakages

Our first aim is to verify that the magnitude of the absorption rates W_f given in Table I is reasonable. This can be easily made by studying the behavior of cycling transitions. Let us consider a laser LD1 in the pumping region tuned to the $F=3\rightarrow F'=2$ transition and σ polarized. No change among populations of the $F=4$ ground-state level would be expected in the absence of leakages. Consequently, the detected fluorescence light of a laser LD2 tuned to the $F=4\rightarrow F'=5$ transition would show no modification at all whether LD1 is "on" or "off." Nevertheless, the observed fluorescence light increases as the excitation power of the laser diode LD1 increases, indicating an increase of the $F=4$ ground-state population due to the simultaneous excitation of the $F=3\rightarrow F'=3$ transition 150 MHz apart from the $F=3\rightarrow F'=2$ transition.

Figure 9 shows the observed population increase. Using the model of Sec. II and the data of Table I, the population increase of the $F=4$ level is calculated to yield the solid curve in Fig. 9. It agrees very well with the experimental results.

Similarly, Fig. 10 shows the observed and calculated variation of the $F=4$ level population when the atoms in the pumping region experience a polarized laser light tuned to the $F=4\rightarrow F'=5$ transition. In this case the influence of the $F=4\rightarrow F'=4$ transition, which is about 251 MHz apart from the $F=4\rightarrow F'=5$ transition, is evident. It may be noted that the $F=4\rightarrow F'=5$ transition exhibits less leakage than the $F=3\rightarrow F'=2$ transition, corresponding to its larger separation from neighboring transitions.

The above results show that leakages have important effects as long as cycling transitions are concerned. Indeed, cycling transitions do not define a two-level system: the pumping which does occur in the presence of an excited neighboring transition provides a transfer of population among the ground-state levels. Atoms are lost from the point of view of a two-level system.

Let us consider now the effects of leakages when a pumping transition, the $F=3\rightarrow F'=3$ one with a σ-polarized light for instance, is considered (see Fig. 5). The fraction of atoms for which the $F=3\rightarrow F'=2$ way is open as resulting from the leakage effect, come back

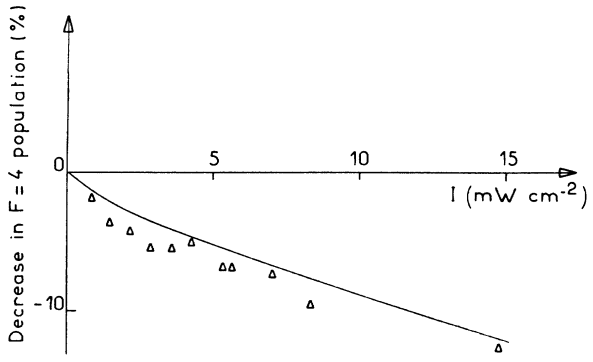

FIG. 10. Same as Fig. 9, but the laser is tuned to the $F=4\rightarrow F'=5$ transition.

only in the starting $F=3$ level by spontaneous emission, and are quickly pumped again. Therefore the leakage effect introduces only a weak delay in the pumping and furthermore, no significant modification in the population of the $m_F=0$ ground-state sublevels occurs. As predicted by the model, the fractional population difference change is less than 5 parts in 10^4. Two main consequences can be drawn from this fact. Firstly, as an appreciable population leakage during the pumping process is observed only when cycling transitions are considered, experiments enable us to verify only the first, second, and fourth values of W_f reported in Table I.[22] Secondly, increase of the pumping time may result from the leakage effect and it may become significant in a two-laser pumping scheme.

There are two alternative means of reducing the leakage effect. The first one consists in decreasing the laser intensity. But this is detrimental to the pumping efficiency and to the fluorescence level. The second, preferred one, makes use of higher spectral purity lasers, whose linewidth is of the order of the natural linewidth.

B. Pumping efficiency

In order to compare theory and experiment quantitatively, it is necessary to cast the calculated results concerning the population of the $m_F=0$ ground-state levels in a form suited to the comparison with the experimental results. For that purpose, one needs to know the value of the fluorescence signal emitted in the detection region. During the interaction time T, it is given by

$$\mathcal{F}=\int_0^T \Gamma\left[\sum_i n_{e_{1i}}+\sum_j n_{e_{2j}}\right]dt \ . \tag{6}$$

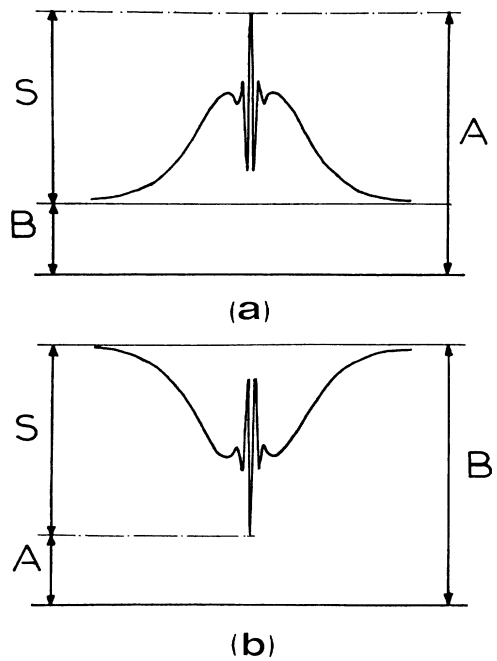

FIG. 11. Schematic Ramsey patterns and definitions of the quantities A, B, and S. (a) Positive case. (b) Negative case.

To obtain the amplitude of the Ramsey microwave resonance signal pictured in Fig. 11(a), we have calculated $\mathcal{F}$ in two circumstances: firstly when the microwave excitation is kept on resonance, in which case we set $\mathcal{F}_{\text{on}}=A$, secondly when the microwave excitation is off so that we have $\mathcal{F}_{\text{off}}=B$, where B characterizes the fluorescence background.

The calculation of the signal level A requires the introduction of the $\Delta F=1$, $\Delta m_F=0$ microwave transition probability at resonance. It was chosen equal to 0.75.[15] This is a reasonable value which corresponds to the optimal transition probability taking into account a Maxwellian velocity distribution in the atomic beam.

The useful signal S is the difference $A-B$. It will be used to compare different pumping schemes with the experimental signals observed at resonance.

1. One-laser scheme

Values predicted when the laser intensity is 10 mW cm^{-2} are reported in Table II. They are the population difference Δn, the fluorescence background B, and the signal S. For purpose of comparison the theoretical and experimental signals are normalized to the largest one, obtained with the $(3\rightarrow 3,\sigma)$ transition. We have verified that the observed backgrounds are negligible and that consequently, the pumping is completely achieved. The experimental values of the relative signal amplitude, $(S/S_{\text{max}})_{\text{expt}}$, agree well with the calculated ones, allowing us to conclude that the Δn values, predicted by the model, are effectively obtained.

2. Two-laser scheme

Table III reports the theoretical predictions and the experimental results as defined above. The laser intensity is assumed to be equal to 3 mW cm^{-2} and the interaction time to 20 μs. As we have two pumping lasers, the detection is possible by either of them. A first possibility consists in using the laser tuned to a transition starting from an empty ground-state level. For instance, it is the $(4\rightarrow 4,\sigma)$ configuration, as indicated in the first line of Table III. The calculated and observed background fluorescence signals are then a test of the depopulation of the level considered. The recorded signal as shown in Fig. 11(a) is superimposed on the background fluorescence signal. The second possibility is to use the laser tuned to the $F'-F=0$ transition with the π polarization changed into a σ one. The fluorescence background is thus very large and the signal S appearing as a negative signal is shown in Fig. 11(b). Although this detection technique shows a drawback from the point of view of the signal-to-noise ratio, we present the related results as a check of the available population difference.

Concerning fluorescence backgrounds, we have first verified that their relative experimental values are in good agreement with the predicted ones. Secondly, we may note that fluorescence backgrounds obtained with the appropriate detection laser are important compared to the one-laser pumping scheme, indicating thus an incomplete hyperfine pumping. This occurs even in the two best pumping schemes as predicted by the model.

TABLE II. Results in the case of one-laser pumping. Δn is the fractional population difference between the $m_F=0$ ground-state sublevels. B and S are the calculated background and signal amplitudes. S_{max} is the signal obtained with the $(3\rightarrow 3,\sigma)$ scheme. $(S/S_{max})_{expt}$ is the experimental value of the relative signal amplitude. The laser intensity I is 10 mW cm^{-2}, the interaction time T is 3 μs, and the laser linewidth $\Delta\nu_L$ is 25 MHz.

F	F'	Polarization	Δn (%)	B (photon atom^{-1})	S^a (photon atom^{-1})	S/S_{max}	$(S/S_{max})_{expt}$
3	3	π	−8.5	0.02	0	0	0
3	3	σ	12.2	0	0.36	1	1
3	4	π	13.7	0	0.17	0.47	0.47
3	4	σ	9.9	0	0.12	0.33	0.36
4	3	π	−12.1	0	0.12	0.33	0.4
4	3	σ	−15.4	0	0.15	0.41	0.6
4	4	π	2.5	0.04	0	0	0
4	4	σ	−15.5	0	0.28	0.77	0.78

[a]The calculated signal S is a mean value of the number of fluorescence photons referred to the initial atomic beam population and assuming a microwave transition probability equal to 0.75. The actual number β of photons which are emitted in the detection region by an atom in a given $m_F=0$ ground-state sublevel is $\beta=S/(\Delta n 0.75)$. For example, in the $(3\rightarrow 3,\sigma)$ scheme, each atom emits 3.9 photons in the detection region.

Table III shows that typical values are 0.11 photon/atom in the two above-mentioned cases and more important values can be reached when other schemes are chosen. As a matter of fact, with an interaction time equal to 20 μs, the laser-diode intensity is not sufficient to bring all atoms in one of the $m_F=0$ ground-state sublevels. Considering, now, the signal amplitude, comparison of the two last columns of Table III indicates that the experimental and calculated signal values agree reasonably well whatever the detection scheme is, except for the $(3\rightarrow 3,\sigma;4\rightarrow 4,\pi)$ configuration. In this last case, experimental signals are weaker than expected. This fact could be explained invoking a population leakage due to the simultaneous excitation of the $3\rightarrow 3$ and $3\rightarrow 2$ transitions. It could then result in an increase of the pumping time. As the laser intensity is not sufficiently large to populate completely the $F=4$ level, this delay in the pumping would give an effective population difference smaller than the predicted value of 68.1%.

To conclude, it appears that the $(3\rightarrow 3,\pi;4\rightarrow 4,\sigma)$ and the $(3\rightarrow 3,\pi;4\rightarrow 3,\sigma)$ schemes are the most appropriate to achieve an efficient pumping and to concentrate almost all atoms in the $F=3, m_F=0$ sublevel.

VI. CONCLUSION

In this paper we have presented the results of a theoretical and experimental study of the optical pump-

TABLE III. Results in the case of two-laser pumping. Optical pumping is performed with two lasers. One of them is used for optical detection. The physical quantities are defined in Table II. S_{max} is obtained when the $(3\rightarrow 3,\pi;4\rightarrow 4,\sigma)$ scheme is used for pumping and the $(3\rightarrow 3,\sigma)$ one for detection. $I=3$ mW cm^{-2}; $T=20$ μs; $\Delta\nu_L=25$ MHz.

Pumping				Detection						
F	F'	Polarization	Δn (%)	F	F'	Polarization	B (photons atom^{-1})	S^a (photons atom^{-1})	$\lvert S/S_{max}\rvert$	$(S/S_{max})_{expt}$
3	3	π	−89.1	4	4	σ	0.11	1.60	0.60	0.55
4	4	σ		3	3	σ	3.8	−2.67	1	1
3	3	π	−84.2	4	3	σ	0.11	0.84	0.31	0.37
4	3	σ		3	3	σ	3.7	−2.52	0.94	0.95
3	4	π	81.9	3	4	π	0.07	1.05	0.39	0.39
4	4	π		4	4	σ	2.3	−1.47	0.55	0.54
3	3	σ	68.1	3	3	σ	0.51	2.04	0.76	0.57
4	4	π		4	4	σ	2.1	−1.2	0.45	0.36
3	4	σ	52.9	3	4	σ	0.29	0.68	0.25	0.23
4	4	π		4	4	σ	1.99	−0.95	0.36	0.35
3	3	π	−46.1	4	3	π	0.01	0.47	0.18	0.20
4	3	π		3	3	σ	1.90	−1.38	0.51	0.54
3	3	π	−33.4	4	4	σ	0.81	0.6	0.22	
4	4	π		3	3	σ	2.61	−0.99	0.37	0.43

[a]Same remark as in Table II.

ing in a cesium beam in the case where the laser linewidth is large compared to the cesium natural linewidth. Two main conclusions can be drawn. The first one is that leakages occurring during the pumping cycle of a cesium beam can be adequately described with a rate equations model. It has been shown that their effect is specifically important on the cycling transitions which cannot be described by a two-level approximation any longer. The second conclusion is that the use of two lasers results in a good optical pumping efficiency provided that the laser-excited transitions are appropriately chosen. The improvement of the population difference of the $m_F=0$ ground-state sublevels and thus, of the signal amplitude, compared to the one-laser schemes, allows us to consider that this technique is valuable for the state selection in a cesium beam. Moreover, the agreement between predicted and observed values of the fluorescence signals gives confidence in the possibility of applying the optical pumping and optical detection methods to high-performance cesium beam frequency standards.

A significant improvement of the already large population difference achieved can be obtained with laser diodes having a narrower linewidth.[23] In that case the laser intensity is higher and leakages on neighboring transitions are reduced.

ACKNOWLEDGMENTS

The authors wish to thank Dr. Audoin for his deep interest in this work and for many stimulating discussions and comments on this article. They are grateful to P. Petit, D. Guitard, and J. Dupont for efficient technical assistance. This work was supported in part by the Groupement d'Intérêt Public "Temps-Fréquence" and the "Bureau National de Métrologie." The Laboratoire de l'Horloge Atomique is "Equipe de Recherche du Centre National de la Recherche Scientifique associée a l'Université Paris-Sud."

APPENDIX A

The spontaneous emission rates $A_{e_i \to f_k}$ between the cesium D_2 Zeeman sublevels e_i and f_k are given by the relation

$$A_{e_i \to f_k} = a_{e_i \to f_k} \Gamma \ .$$

The relative transition probabilities $a_{e_i \to f_k}$ are tabulated[19] in Table IV.

TABLE IV. Relative transition probabilities of the cesium D_2-line Zeeman sublevels.

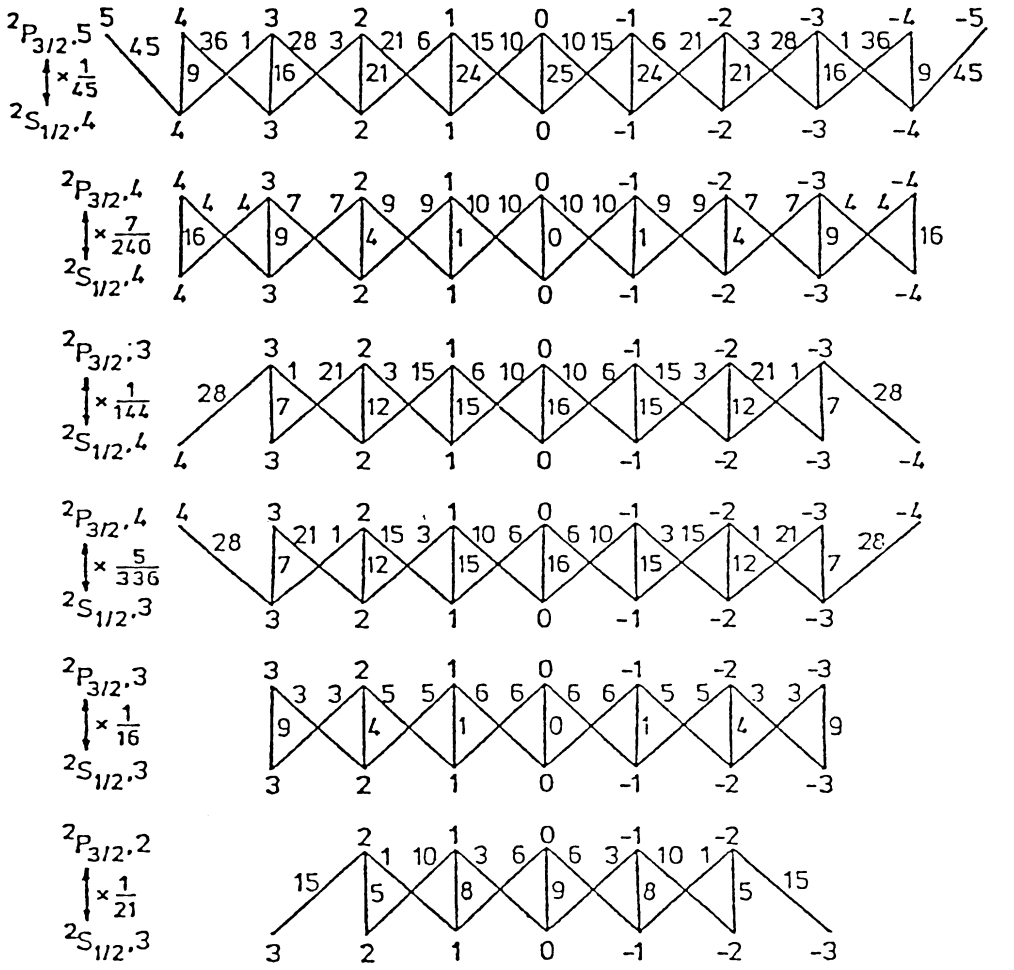

APPENDIX B

When the excited levels of the two transitions involved in a two-laser pumping scheme are the same, the evolution of the population n_{e_i} and n_{f_k}, n_{g_l} of the excited- and ground-state sublevels are given by the following equations:

$$\frac{dn_{e_i}}{dt} = \sum_l W_{g_l \to e_i} n_{g_l} - \sum_l W_{e_i \to g_l} n_{e_i} + \sum_k W_{f_k \to e_i} n_{f_k} - \sum_k W_{e_i \to f_k} n_{e_i} - \Gamma n_{e_i} ,$$

$$\frac{dn_{f_k}}{dt} = - \sum_i W_{f_k \to e_i} n_{f_k} + \sum_i W_{e_i \to f_k} n_{e_i} + \sum_i A_{e_i \to f_k} n_{e_i} ,$$

$$\frac{dn_{g_l}}{dt} = - \sum_i W_{g_l \to e_i} n_{g_l} + \sum_i W_{e_i \to g_l} n_{e_i} + \sum_i A_{e_i \to g_l} n_{e_i} .$$

---

*Present address: European Southern Observatory, Karl-Schwarzschild-Strasse, D-8046 Garching bei München, Federal Republic of Germany.

†Also at Compagnie d'Electricite' et de Piezoélectricité, 44 avenue de la Glacière, 95100 Argenteuil, France.

‡Also at Laboratoire Primaire du Temps et des Fréquences, 61 avenue de l'Observatoire, 75014 Paris, France.

§Author to whom correspondence should be addressed.

[1]W. Dreves, H. Jänsch, E. Koch, and D. Fick, Phys. Rev. Lett. **50**, 1759 (1983).

[2]H. Kleinpoppen, Adv. At. Mol. Phys. **15**, 423 (1979).

[3]G. Avila, P. Gain, E. de Clercq, and P. Cerez, Metrologia **22**, 111 (1986).

[4]C. Fabre,Y. Kaluzny, R. Calabrese, L. Jun, P. Goy, and S. Haroche, J. Phys. B **17**, 3217 (1984).

[5]W. D. Philips and H. Metcalf, Phys. Rev. Lett. **48**, 596 (1982).

[6]S. Chu, L. Hollberg, J. E. Bjorkholm, A. Cable, and A. Ashkin, Phys. Rev. Lett. **55**, 48 (1985).

[7]R. N. Watts and C. E. Wieman, in *Laser Spectroscopy VII,* edited by T. W. Hänsch and Y. R. Shen (Springer-Verlag, Berlin, 1985), pp. 20–21.

[8]A. Aspect, J. Dalibard, A. Heidmann, C. Salomon, and C. Cohen-Tannoudji, Phys. Rev. Lett. **57**, 1688 (1986).

[9]R. N. Watts and C. E. Wieman, Opt. Commun. **57**, 45 (1986).

[10]J. L. Picque, Metrologia **13**, 115 (1977).

[11]A. Kastler, J. Phys. Radium **11**, 255 (1950).

[12]M. Arditi and J. L. Picque, J. Phys. Lett. **41**, L379 (1980).

[13]L. L. Lewis and M. Feldman, in *Proceedings of the 35th Annual Symposium on Frequency Control,* Philadelphia, 1981 (Electronic Industries Assn. Washington, D.C., 1981), pp. 612–624.

[14]L. S. Cutler, United States Patent 4, 425, 653.

[15]N. F. Ramsey, *Molecular Beams* (Clarendon, Oxford, 1956).

[16]C. Cohen-Tannoudji, in *Atomic Physics IV,* edited by G. zu Putlitz, E. W. Weber, and A. Winnacker (Plenum, New York, 1975), pp. 589–614.

[17]E. de Clercq, M. de Labachelerie, G. Avila, P. Cerez, and M. Tetu, J. Phys. (Paris) **45**, 239 (1984).

[18]To simplify the notation, a one-laser pumping scheme in which the laser is tuned to the $F=3 \to F'=4$ transition and σ polarized, for instance, is labeled $(3 \to 4, \sigma)$. Similarly, a two-laser pumping scheme labeled $(3 \to 4, \sigma; 4 \to 4, \pi)$ means that the first laser is tuned to the $F=3 \to F'=4$ transition and σ polarized, while the second one is tuned to the $F=4 \to F'=4$ transition and π polarized.

[19]M. Arditi, I. Hirano, and P. Tougne, J. Phys. D **11**, 2465 (1978).

[20]J. J. McClelland and M. H. Kelley, Phys. Rev. A **31**, 3704 (1985).

[21]V. I. Balykin, Opt. Commun. **33**, 31 (1980).

[22]Unfortunately it is difficult to measure the influence of leakage on lines distant by 200 MHz, corresponding to the third value reported in Table I, because the two simultaneously excited transitions are both pumping transitions: such is the case on the one hand of the $3 \to 3$ and $3 \to 4$ transitions and of the $4 \to 4$ and $4 \to 3$ ones on the other hand.

[23]M. de Labachelerie and P. Cerez, in *Proceedings of the 1986 European Conference on Optics, Optical Systems and Applications, Firenze, 1986,* edited by S. Sottini and S. Trigari, Vol. 701, pp. 182–184.